

---

Proceedings of the XXIV International School of Semiconducting Compounds, Jaszowiec 1995

# WEAKLY DILUTED MAGNETIC CdTe/Cd<sub>1-x</sub>Mn<sub>x</sub>Te SEMICONDUCTOR STRUCTURES GROWN BY MBE\*

T. WOJTOWICZ, G. KARCZEWSKI AND J. KOSSUT

Institute of Physics, Polish Academy of Sciences  
Al. Lotników 32/46, 02-668 Warszawa, Poland

In this paper we review the results of our effort to grow layers and low-dimensional structures containing Cd<sub>1-x</sub>Mn<sub>x</sub>Te diluted magnetic semiconductor with relatively high values of Mn molar fraction  $x$ . A high quality of the structures grown so far is demonstrated by making use of results of several selected experiments. In the case of the epilayers having bulk-like thickness with  $x \geq 0.7$  we discuss, in particular, the magnetic phase diagram as well as we report on collective spin excitation (magnons) observed in Raman scattering experiments. The discussion of the growth of different quantum wells, including rectangular, digital, parabolic and wedge quantum wells, is accompanied by a brief overview of their optical and magneto-optical properties. These results include first measurements concerning magnetic polarons in quantum wells embedded in Cd<sub>1-x</sub>Mn<sub>x</sub>Te barriers with  $0.4 \leq x \leq 0.8$ . Finally, we report on the present status of the search for dimensional effects in the spin-glass phase performed with the use of our specially designed superlattice structures.

PACS numbers: 73.20.Dx, 78.55.Et

## 1. Introduction

Experiments on bulk crystals of diluted magnetic semiconductor (DMS) system Cd<sub>1-x</sub>Mn<sub>x</sub>Te have been limited to Mn concentration  $x$  below, approximately, 0.7. The reason for this limitation is that equilibrium growth techniques can produce these materials with a single crystal phase only in such composition range. On the other hand, the region of higher mole fractions ( $x \geq 0.7$ ) is particularly interesting as far as magnetic properties of these materials are concerned. Zinc-blende (ZB) Mn chalcogenides represent unique examples of Heisenberg fcc antiferromagnets with strongly dominant, nearly isotropic nearest-neighbor exchange interaction. The study of the influence of weak dilution, strain and dimensionality on these systems is of primary scientific interest [1].

---

\*This work is supported in part by the State Committee for Scientific Research (Republic of Poland) through grant PBZ-ZO11/P4/93/01.

Recent progress in non-equilibrium growth techniques, especially in molecular beam epitaxy (MBE), made possible a realization of DMS materials with  $x$  exceeding 0.7 required for such studies. Although the first successful growth of ZB MnTe by MBE was reported by Durbin et al. [2] already several years ago, the number of papers devoted to structures containing  $\text{Cd}_{1-x}\text{Mn}_x\text{Te}$  with high Mn molar fractions has been still very limited. This is because the growth of structures with high  $x$ , even in the case of MBE, is much more challenging than those with small  $x$ .

In this paper we report on our effort to obtain such structures with the use of an EPI 620 MBE machine in the Institute of Physics of the Polish Academy of Sciences in Warsaw. The structures include single-crystal cubic MnTe films with a "bulk-like" thickness (up to 8  $\mu\text{m}$  — the thickest ZB MnTe ever grown),  $\text{Cd}_{1-x}\text{Mn}_x\text{Te}$  single-crystal films in previously inaccessible Mn concentration region  $0.7 \leq x \leq 1$ , as well as various low dimensional structures composed of these materials. We succeeded in producing high quality quantum wells (QWs) and superlattices (SLs) with a very strong quantum confinement. We were able to grow also more complicated structures like digital magnetic QWs (i.e., QWs in which the well material is itself a short period SL), wedge QWs (where QW-width changes in one of the two in-plane directions perpendicular to the growth axis) and, finally, parabolic QWs (where quantum confining potential assumes a parabolic shape). The use of hybrid GaAs/ZnTe/CdTe substrates allowed us to produce specimens with volumes large enough for experiments, such as magnetization measurements, that require particularly large samples.

In this paper we will give a review of several results obtained on our samples. These include first studies of the magnetic phase diagram of  $\text{Cd}_{1-x}\text{Mn}_x\text{Te}$  for high  $x$ , observation of spin-wave excitation (magnons) by Raman scattering, results of a search for dimensional effects in spin-glass transition in  $\text{Cd}_{1-x}\text{Mn}_x\text{Te}/\text{CdTe}$  SLs, as well as studies of magnetic polarons in QWs.

## 2. Epilayers

A series of  $\text{Cd}_{1-x}\text{Mn}_x\text{Te}$  epilayers with  $0.4 \leq x \leq 1$  and with bulk-like thickness (from 3 to 8  $\mu\text{m}$ ) have been grown on (100)GaAs substrates [3]. They were, subsequently, used to study the magnetic phase diagram in the range of high Mn molar fractions. Measurements of the magnetization were performed with a SQUID magnetometer on "sandwich" samples prepared from about 1  $\text{cm}^2$  of the initial material. Preparation of these sandwiches consisted of reducing GaAs substrate thickness to about 100  $\mu\text{m}$ , breaking the specimens into  $4 \times 4 \text{ mm}^2$  squares and, finally, gluing them in a stack.

In the case of pure ZB MnTe, Sawicki et al. [4] studied the magnetization in two configurations, with the magnetic field perpendicular or parallel to the growth axis. The experiments were done on (100) as well as on (111) oriented epilayers. No differences in the values of the magnetization were observed indicating that neither the growth orientation nor a residual strain have any influence on the magnetic properties seen by SQUID. The critical temperature for the transition between paramagnetic and antiferromagnetic phase in ZB MnTe obtained from these experiments,  $T_F = 67 \text{ K}$ , is in perfect agreement with the value obtained by

Giebułtowitz et al. [1] from neutron scattering. In contrast, the transition temperature obtained previously from SQUID measurements by Ando et al. [5] was slightly lower.

The fact that we were able to grow ZB MnTe as thick as 8  $\mu\text{m}$  (which is to our knowledge the thickest cubic MnTe film ever grown by MBE) suggests that ZB phase may actually be the stable phase of MnTe grown at low temperatures, contrary to previous suggestions that ZB phase is unstable, and only becomes stabilized by cubic substrates provided that the thickness of the film does not exceed a certain critical value.

The resulting phase diagram for Cd<sub>1-x</sub>Mn<sub>x</sub>Te in the entire composition range [6, 4] is presented in Fig. 1. We have plotted here also the data obtained previously on bulk samples [7, 6]. The boundary at  $x = 0.6$  between the spin-glass and the antiferromagnetic phases has been proposed by Gałazka et al. on the basis of specific heat measurements [7]. Later, neutron diffraction studies have put a question mark on the validity of this distinction. Here, we note that the supposedly different magnetic behavior of these possible two phases as seen by SQUID

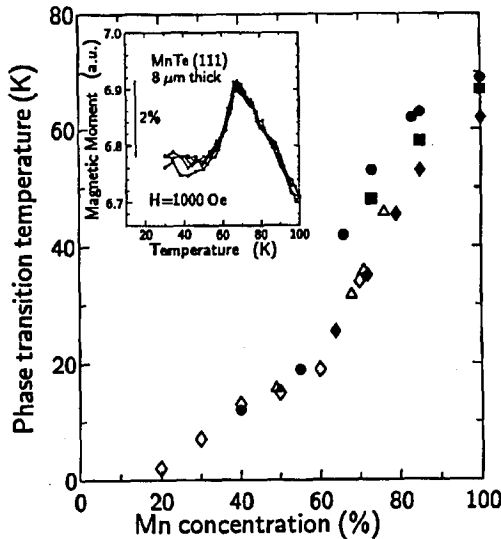


Fig. 1. The magnetic phase transition temperature in Cd<sub>1-x</sub>Mn<sub>x</sub>Te. Data marked by full symbol points are for MBE-grown samples: circles and squares represent data from magnetization measurements on our samples in the SQUID apparatus by Pietruczanis et al. [6] and Sawicki et al. [28], respectively, diamonds show the data of Ando et al. [29] obtained from magnetic circular dichroism experiments. Open diamonds and triangles represent magnetization data for bulk crystals by Gałazka et al. [7] and Pietruczanis et al. [6]. The inset shows the cusp-like feature observed in a thick MBE-grown film of cubic MnTe at the transition temperature.

manifests itself as a much steeper increase in  $T_F$  with increasing Mn composition for  $x > 0.6$ . Another observation is that, although no difference between epilayers and bulk crystals can be noticed for  $x < 0.6$ ,  $T_F$  for epilayers with large  $x$  is somewhat higher than that of the bulk materials with a corresponding  $x$ . These facts have not been understood properly yet. It is possible that the latter observation is due to a different type of clustering of Mn ions taking place during MBE at the growth temperatures of about 300°C, much lower than those used for growth of bulk crystals. However, more studies are required to clarify the problem.

$\text{Cd}_{1-x}\text{Mn}_x\text{Te}$  epilayers have also been recently the subject of Raman scattering experiments which reveal the existence of collective spin excitations, called magnons, in both pure ZB MnTe and in the mixed crystals with  $x > 0.6$  [8]. The energies of the magnon mode are consistent with those obtained by extrapolation of the results obtained by other researchers on bulk samples containing smaller amounts of Mn [9]. Softening of the magnon mode with an increasing temperature until their disappearance at the critical temperature (equal to that measured by SQUID) is also observed, corroborating their identification.

Studies of magneto-optical properties of  $\text{Cd}_{1-x}\text{Mn}_x\text{Te}$  epilayers with large Mn mole fractions deposited on GaAs were found to be quite difficult in the reflection configuration [10]. Therefore, we have recently grown first samples of cubic MnTe on transparent (111)BaF<sub>2</sub> substrates [11]. It was then demonstrated by direct measurements of the absorption edge in a transmission experiment that the energy gap of MnTe is greater than 3 eV, thus proving again the zinc-blende structure of these samples (the energy gap of the hexagonal variation of MnTe is known to be considerably smaller, approximately 1.3 eV).

### 3. Quantum wells

Quantum wells with weakly diluted MnTe barriers are not only interesting because of the unique magnetic properties of the barrier material but also because they are characterized by a very strong quantum confinement. The latter property can have many interesting implications, including a very strong anisotropy in an external magnetic field [12].

High quality quantum wells and multiple QW structures were grown in our laboratory in the full range of Mn composition in the barriers. Majority of our growth processes have been performed on hybrid (100)GaAs/ZnTe/CdTe substrates with a typical CdTe buffer thickness of about 3.5  $\mu\text{m}$ . Both a regular MBE growth mode and atomic layer epitaxy (ALE) growth mode could be used to produce CdTe QW. These two growth methods yielded structures having a similar photoluminescence quality (see Fig. 2). In the MBE growth mode of CdTe wells (or  $\text{Cd}_{1-x}\text{Mn}_x\text{Te}$  barriers) both Cd and Te fluxes (or Cd, Mn and Te fluxes) impinge simultaneously onto the substrate, and a precise control of the width of QW is achieved only after a careful calibration of the growth rate. This calibration is done by monitoring the period of intensity oscillations of characteristic fragments (the specular spot, in most of the cases) of reflected high energy electron diffraction (RHEED) patterns. The flux dependent growth rate used in our processes was chosen to be in the range 0.12–0.7  $\mu\text{m}/\text{h}$ . In the ALE mode, used by us to grow CdTe wells only, the fluxes of Cd and Te impinge alternatively on a substrate,

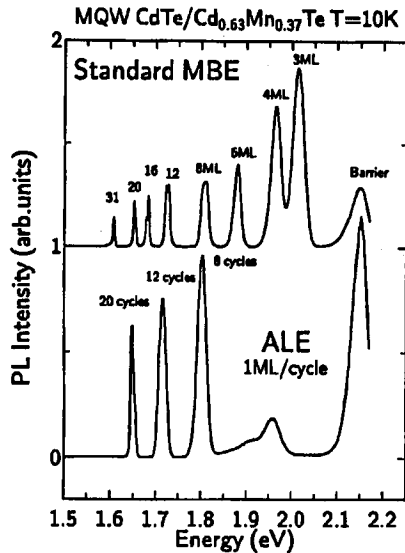


Fig. 2. Luminescence from isolated quantum CdTe wells surrounded by Cd<sub>1-x</sub>Mn<sub>x</sub>Te barriers. Upper trace — the sample grown by standard MBE, lower trace — the sample grown by ALE. Each ALE cycle corresponds to one monolayer grown by MBE.

with some dead time in between allowing for re-evaporation of excessive atoms from the surface.

In the ALE growth mode the growth rate depends primarily on the substrate temperature. If the temperature is chosen correctly (i.e., in a proper range) a single monolayer per growth cycle is deposited [13], as demonstrated in Fig. 2. In this figure we compare the photoluminescence energy from a multiple quantum well structure produced by the regular MBE with that from a structure in which three QWs were produced by 20, 12 and 8 Cd/Te ALE cycles, respectively. There is good agreement between the PL energies in ALE-grown QWs and those in regular QWs. This data indicate also that the quality of the QW luminescence is determined mainly by roughness of the interface with Cd<sub>1-x</sub>Mn<sub>x</sub>Te barriers. In order to decrease luminescence line width it is then necessary to improve first the interface smoothness. This, hopefully, can be done with the use of ALE combined with pulsed Mn flux during the growth of the barriers.

A high precision of the growth of QWs with a required width is demonstrated in Fig. 3, where PL peak energies observed in a set of multiple QWs with nominal thicknesses 4, 6, 12 and 30 monolayers (ML) containing various Mn amount in the barriers are compared with a theoretical calculation done without any adjustment of QW width [14]. Small scatter of the data around theoretical lines can be explained in terms of slightly different Mn profiles across the interfaces between barriers and wells in each particular sample. This composition profile of the interface can be characterized by a method which takes advantage of an enhanced spin splitting of the states in QW with non-abrupt interfaces with DMS barriers [15].

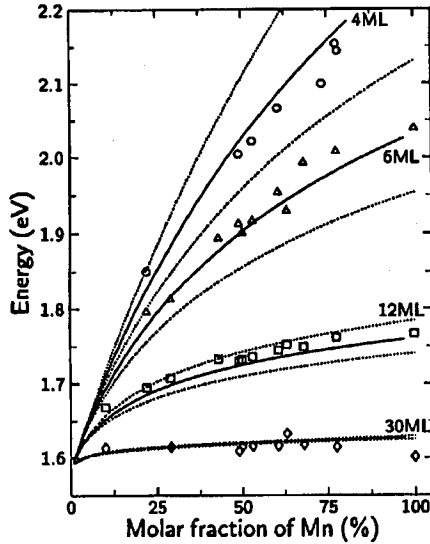


Fig. 3. Energy of the luminescence from CdTe quantum wells as a function of Mn molar fraction  $x$  of thick  $\text{Cd}_{1-x}\text{Mn}_x\text{Te}$  barriers. The nominal width of the wells is given in the figure. Solid lines represent values calculated for the nominal thickness of the wells while dotted lines give the values calculated assuming that the wells differ in widths by ( $\pm 1$ ) monolayer from the nominal thickness. Exciton binding energy was estimated within the fractional dimension approach [14].

The value of the “Mn-interdiffusion length” obtained by this method in our samples is of the order of 1 ML [16]. Such value is typical for good quality structures grown at similar substrate temperatures in other laboratories [15].

Our  $\text{Cd}_{1-x}\text{Mn}_x\text{Te}/\text{CdTe}$  QW structures with  $0.4 \leq x \leq 0.8$  were used to extend earlier studies of two-dimensional magnetic polarons [18] into the previously unexplored region of high Mn molar fractions. The magnetic polaron energies and formation times were measured by cw- and time-resolved photoluminescence under selective excitation [19]. In agreement with previous findings, the polaron formation time depends predominantly on the Mn content, and decreases with increasing  $x$ . On the other hand, a very interesting new finding of this study is that the magnetic polaron formation leads to an appearance of an additional line in the photoluminescence excitation spectra, not observed previously for lower  $x$  values. Moreover, the new line can also be used to determine the Zeeman splitting of the heavy hole exciton with a precision greater than that possible in direct measurement of the magnetic field dependence of the heavy hole exciton photoluminescence line.

Energies of the magnetic polaron measured for high Mn composition were found to be larger than those for Mn contents  $x \leq 0.4$ . That is just opposite to what one might expect (since higher Mn composition means stronger Mn–Mn antiferromagnetic interaction and, therefore, lower magnetic polaron energy). An

analysis of possible mechanisms that could be responsible for the above observation leads to the conclusion that large polaron energies sensitively reflect the Mn profile at the interface. Studies of the magnetic polaron energy may, therefore, be used as a method of interface profile characterization in samples having high- $x$  material, in addition to previously proposed and commonly used method based on an enhanced Zeeman splitting [15]. In fact, the conclusions obtained from the magnetic polaron studies concerning the lack of interface sharpness are confirmed by the latter method.

Very large band gap discontinuity, inherent for high  $x$  structures, together with internal strain, causes a considerable heavy hole-light hole splitting. As a consequence, a very strong anisotropy between the suppression of polaron formation by an external magnetic field in Faraday and Voigt geometry was found. This anisotropy was qualitatively described by model calculations [19].

Apart from regular rectangular wells we have recently grown new structures called digital magnetic QWs (DMQW). In these structures the well material is itself a short period superlattice (SPSL) composed of alternating diluted magnetic semiconductor and nonmagnetic layers each only a few monolayers thick [20]. The realization of this new QWs has been confirmed by direct transmission electron microscopy studies, showing distinct CdTe and Cd<sub>1-x</sub>Mn<sub>x</sub>Te layers inside the QW material. Novel structures of this type can be useful in a variety of studies including studies of the barrier-well interface sharpness and low-dimensional magnetism. For example, DMQWs with SPSL comprised of one ML of cubic MnTe alternated with  $n$  MLs of CdTe grown on a (100) plane, and immersed in MnTe barriers, provides a system suitable for studying 2D antiferromagnetism by optical methods. Also, with an increase in  $n$ , i.e., with increasing separation between magnetic layers, one can try to study the crossover from 3D to 2D magnetism, and to obtain information on the range of the antiferromagnetic coupling between magnetic ions. The advantage of DMQW is that the 2D magnetic material is inside the well and that only several MLs are sufficient to make a useful structure. This not only saves effusion cell shutter lifetime, but also allows one to grow structures of better quality and reproducibility than is the case with thick structures such as these required for SQUID magnetization measurements.

The digital method used to grow DMQWs can easily be modified to allow the growth of QWs with an arbitrary shape of the confining potential. In order to obtain the required shape, the growth of a quantum well is divided into short steps. For each step the manganese effusion cell is open for the time needed to obtain a given (required by the assumed shape) value of Mn composition. For example, if the Mn molar fraction needed for a particular step is equal to 25% then the Mn cell is to be open for 1/4 of the time required to grow this step [21]. The step can be as small as one monolayer provided that the growth rate is low enough and the shutter closing time is very short. In our MBE system this time is below 0.1 s while the time required to grow one ML can be easily extended to over 8 s. Thus, a relatively small error in the profiling of the composition can be achieved, at least for intermediate values of the molar fraction. This has been demonstrated in our MBE system by the growth of QW during which the Mn-cell was open 1/3 of the time required to grow one ML. The value of Mn mole fraction obtained from PL

energy observed from this structure was 34% (of that in the barriers), in perfect agreement with the expected composition of 33.3%.

One of the most important parameters characterizing semiconductor heterostructure is the value of the valence-band offset  $\Delta E_v$  at the junction between constituent materials. Many different methods have been used to determine this value for CdTe/MnTe system, some taking advantage of the giant spin splitting characteristic for DMS. All of them suffer from a drawback, namely that they involve a fit to some more or less complicated model, typically with more than one fitting parameter. Moreover, in rectangular QWs the level energies are known to be not very sensitive to  $\Delta E_v$ . In parabolic quantum wells, on the other hand, energy-level spacings are directly determined by curvatures of the confining potential [21]. For infinite barrier height, QW energy level spacing for  $i$ -th particle (conduction electron, heavy or light hole) is given by the following formula:

$$E_{ni} = \left( n - \frac{1}{2} \right) \frac{\hbar}{L_z} \left[ \frac{8Q_i \Delta E_g}{m_i^*} \right]^{1/2}, \quad (1)$$

where  $Q_i = \Delta E_i / \Delta E_g$ ,  $\Delta E_g$  is the energy band gap discontinuity at a distance  $\pm L_z/2$  from the center of the well,  $m_i^*$  is the mass of the particle,  $i = e, \text{lh}, \text{hh}$  and  $n = 1, 2, 3, \dots$  being the harmonic oscillator quantum number. Therefore, as already demonstrated by Miller et al. [21] in the case of GaAs-GaAlAs system, parabolic QWs are very useful for the band-offset determination.

In order to make use of this property we grew a set of three parabolic quantum wells with a thicknesses of 41, 62 and 82 ML and the same Mn composition of the barriers,  $x = 0.8$  (as given by the value of the lattice parameter measured by X-ray diffraction). The digital growth method described above was used. Photoluminescence excitation (PLE) spectra obtained on these samples at 10 K are presented in Fig. 4 [22]. In the spectra we can clearly see sets of pronounced, equally spaced peaks, which we interpret as due to  $\text{hh}_n$  to  $e_n$  exciton transitions. In the case of the thickest QW four such transitions were observed ( $n = 1, 2, 3, 4$ ) while for the thinnest — only two. The left-hand side inset in Fig. 4 demonstrates for 82 and 62 ML QWs that the transitions between  $\text{hh}_n$  and  $e_n$  are equally spaced in energy for different  $n$ . This is the first indication that the shape of the confining potential is indeed parabolic. Moreover, as additionally shown by the right-hand side inset in Fig. 4, the energy level separation in our three QWs scales with  $1/L_z$  as expected for parabolic QWs. Having confidence that we are, in reality, dealing with parabolic QWs we determined the valence band offset from the experimental slope of the level separation vs.  $1/L_z$  dependence. Assuming effective masses  $m_{\text{hh}}^* = 0.65$  and  $m_e^* = 0.095$  we obtain for the valence-band offset  $Q_{\text{hh}} = 0.4 \pm 0.1$ . The error reflects the uncertainty in effective mass values only. Our value of the offset is in reasonable agreement with commonly accepted value  $Q_{\text{hh}} = 0.3$ . But, of course, one has to keep in mind that our estimate is based on the assumption of an infinite barrier height. However, we do not expect that a calculation assuming finite barriers will modify the above value of the band offset considerably in view of rather large widths of our parabolic wells.

In studies of QWs that are aimed at a detailed comparison of their properties as functions of the QW width, it is of extreme importance to have all remaining

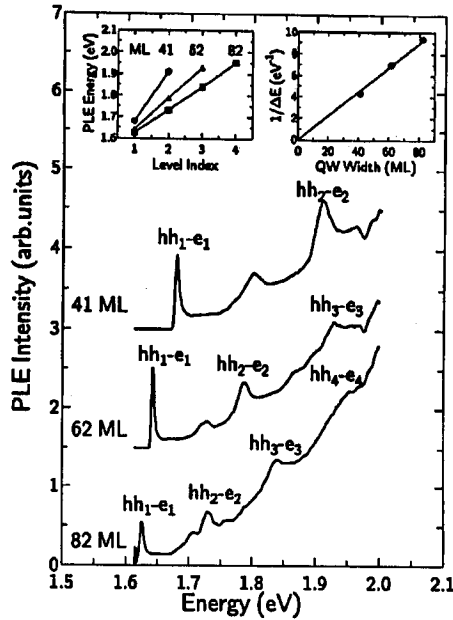


Fig. 4. PLE from three parabolic quantum wells with different thicknesses. The insets show the energy of the optical transitions scales as expected for parabolic potential profiles.

parameters constant. This is not simple to achieve even if one uses a multiple QW structure, because then each particular QW (with a given width) is located at a different distance from the surface (or the substrate) and, therefore, is the subject to slightly different dislocation/strain conditions. This is especially important in the case of structures grown on strongly lattice mismatched substrates, as it is in the case of CdTe/Cd<sub>1-x</sub>Mn<sub>x</sub>Te structures grown on GaAs. On the other hand, if one uses a set of similar structures each containing only a single QW located at the same distance from the surface (substrate) then, for each structure, the barrier composition may easily turn out to be slightly different (it is difficult to ascertain exactly the same growth conditions even in consecutive growth processes). Therefore, for sensitive experiments we propose to use a special design of a QW structure, the so-called "wedge QW". In this type of a structure the width of QW changes continuously in one direction of the QW plane perpendicular to the growth axis. Since the whole structure, containing an entire "set" of QWs, is produced within **one** growth process, all its remaining parameters stay constant. The growth of such structures is achieved in our MBE system in the following way. First, a Cd<sub>1-x</sub>Mn<sub>x</sub>Te buffer is grown on a 5 cm long, 5 mm wide GaAs substrate. Then the substrate rotation is stopped and the growth of CdTe well commences while the main shutter is moved at the same speed in 5.2 mm steps parallel to the longer edge of the substrate. After completion of the quantum well the second barrier is grown while rotating the substrate. Photoluminescence from such sample

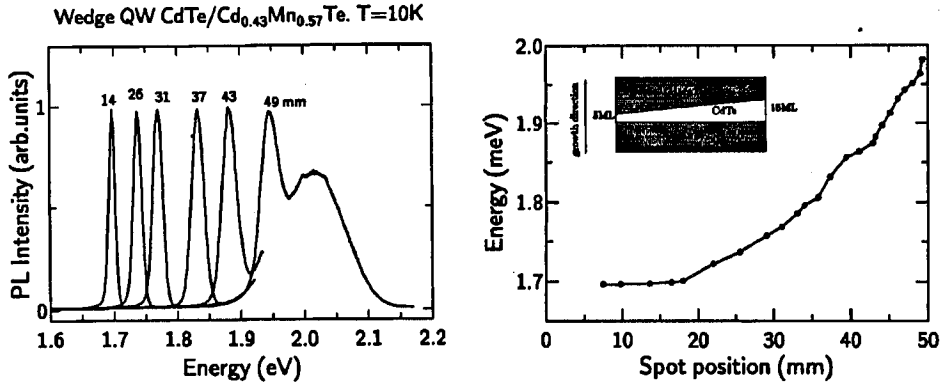


Fig. 5. Photoluminescence intensity of the wedge QW observed for different positions of exciting laser beam on the sample (left part). The right part shows the plot of PL peak energy versus the position of the exciting laser spot.

is presented in Fig. 5. In the left part of the figure one can clearly see that PL peak energy shifts as the exciting laser beam scans the sample. Steps in the PL energy vs. the exciting beam position, shown in the right part of the figure, are only discernible in the region where the well is thinnest. This is related to CdTe flux shadow being not very sharp, because of a large distance between the main shutter and the substrate in our MBE system. Having demonstrated that the wedge QW can be in fact produced we may speculate about possible applications of the wedge QW structures, e.g., for producing "tunable" light sources. In the case of the wedge QW structure such "tuning" would be obtained simply by moving the exciting laser beam along the structure. In principle, it is also possible to pattern an analogous and properly doped structure into a row of luminescent diodes (or lasers), each operating at a different energy. The energy of the light would, then, be chosen by sending current through an appropriate diode.

#### 4. Superlattices

An increased interest in the studies of the influence of reduced dimensionality on magnetic properties observed in recent years stimulated us to grow superlattice structures designed specially to help in the search for dimensional effects in spin-glasses (S-G). A set of four superlattices having the same thickness (16 ML) of CdTe well and differing in the thickness of Cd<sub>0.5</sub>Mn<sub>0.5</sub>Te barriers has been grown by standard MBE on (100)GaAs substrates. The thickness of magnetic layers in successive SLs was reduced from 20, through 15 and 10, down to 5 ML. Sawicki et al. [23] measured (with a SQUID magnetometer) the susceptibility of "sandwich" samples prepared from these SLs. These SQUID data contradict previous results obtained on (111)CdTe/Cd<sub>1-x</sub>Mn<sub>x</sub>Te SLs [24] which seemed to indicate that a 12 ML thick magnetic layer corresponded to a critical thickness for the occurrence of S-G phase in Cd<sub>1-x</sub>Mn<sub>x</sub>Te. In the case of our samples Sawicki et al. observed distinct fingerprints of the spin-glass transition for all studied SLs including that with the thinnest (5 ML) magnetic layers. The observation did not depend

on the orientation of an external magnetic field with respect to the growth axis. Although the values of freezing temperature obtained from thermoremanent magnetization measurements decrease as the thickness of magnetic layers is reduced, the extrapolation to vanishing thickness gives a finite value of  $T_F$  in 1D limit. These conclusions based on the data obtained in SQUID experiments were confirmed in a study of magneto-optical Kerr effect on the very same SLs [25]. Measurements of the frequency dependence of the freezing temperature (from 4 Hz to 30 kHz) did not reveal any qualitatively drastic difference of the behavior of the spin-glass transition from that seen in the bulk material.

## 5. Conclusions

In this paper we tried to give a short review of the effort to grow weakly diluted magnetic CdTe/Cd<sub>1-x</sub>Mn<sub>x</sub>Te semiconductor structures in the Institute of Physics of the Polish Academy of Sciences in Warsaw. This review, because of space limitations, is far from being complete. We have also omitted many interesting aspects of the physics of the systems in question with low  $x$ , e.g., concerning their doping [26], first observation of universal conductivity fluctuations in Cd<sub>1-x</sub>Mn<sub>x</sub>Te quantum wires [27], etc. The reader is referred to several other papers in these Proceedings presenting more results of various types of measurements taken recently on our samples.

## Acknowledgments

We would like to thank Professor A. Mycielski for supplying us with high purity Mn used as a source material for MBE.

## References

- [1] T.M. Giebułtowicz, P. Kłosowski, N. Samarth, H. Luo, J.K. Furdyna, *Phys. Rev. B* **48**, 12817 (1993).
- [2] S.M. Durbin, J. Han, Sungki O, M. Kobayashi, D.R. Menke, R.L. Gunshor, Q. Fu, N. Pelekanos, A.V. Nurmikko, D. Li, J. Goncalves, N. Otsuka, *Appl. Phys. Lett.* **55**, 2087 (1989).
- [3] E. Janik, E. Dynowska, J. Bąk-Misiuk, M. Leszczyński, W. Szuszkiewicz, T. Wojtowicz, G. Karczewski, A.K. Zakrzewski, J. Kossut, *Thin Solid Films*, in press.
- [4] M. Sawicki, S. Kolesnik, T. Wojtowicz, G. Karczewski, E. Janik, M. Kutrowski, A. Zakrzewski, E. Dynowska, T. Dietl, J. Kossut, *Superlattices Microstruct.* **15**, 475 (1994).
- [5] K. Ando, K. Takahashi, T. Okuda, *J. Magn. Magn. Mater.* **104–107**, 993 (1992).
- [6] J. Pietruczanis, W. Mac, A. Twardowski, G. Karczewski, A. Zakrzewski, E. Janik, T. Wojtowicz, J. Kossut, *Material Science Forum*, in press.
- [7] R.R. Gałazka, S. Nagata, P.H. Keesom, *Phys. Rev. B* **22**, 3344 (1980).
- [8] W. Szuszkiewicz, M. Jouanne, E. Dynowska, E. Janik, G. Karczewski, J. Kossut, T. Wojtowicz, *Acta Phys. Pol. A* **88**, (1995), Proc. of this Conf. (Part II).
- [9] See, e.g., *Semiconductors and Semimetals*, Eds. J.K. Furdyna, J. Kossut, Vol. 25, Academic Press, Boston 1988; J. Kossut, W. Dobrowolski, in: *Handbook of Magnetic Materials*, Ed. K.H.J. Buschow, Vol. 7, North-Holland, Amsterdam 1993, Chap. 4.

- [10] A. Stachow, W. Mac, Nguyen The Khoi, A. Twardowski, G. Karczewski, E. Janik, T. Wojtowicz, J. Kossut, *Acta Phys. Pol. A* **88**, (1995), Proc. of this Conf. (Part II).
- [11] E. Janik, T. Wojtowicz, E. Dynowska, J. Bąk-Misiuk, J. Domagała, M. Kutrowski, G. Karczewski, J. Kossut, *Acta Phys. Pol. A* **88**, (1995), Proc. of this Conf. (Part II).
- [12] B. Kuhn-Heinrich, W. Ossau, E. Bangert, A. Waag, G. Landwehr, *Solid State Commun.* **91**, 413 (1994).
- [13] W. Fashinger, *Phys. Scri. T* **49**, 492 (1993).
- [14] M. Kutrowski, K. Kopalko, G. Karczewski, T. Wojtowicz, J. Kossut, *Thin Solid Films*, in press.
- [15] J.A. Gaj, W. Grieshaber, C. Bodin-Deshayes, J. Cibert, G. Feuillet, Y. Merle d'Aubigne, A. Wasiela, *Phys. Rev. B* **50**, 5512 (1994).
- [16] P. Kossacki, Nguyen The Khoi, J.A. Gaj, G. Karczewski, T. Wojtowicz, J. Kossut, K.V. Rao, *Solid State Commun.* **94**, 439 (1995).
- [17] J.A. Gaj, P. Kossacki, Nguyen The Khoi, J. Cibert, W. Grieshaber, Y. Merle d'Aubigne, G. Karczewski, J. Kossut, T. Wojtowicz, in: *Proc. of SPIE Conf. on Integrated Electronics, San Jose, 1995*, in press.
- [18] D.R. Yakovlev, in: *Festkörperprobleme/Advances in Solid State Physics*, Ed. U. Rössler, Vol. 32, Vieweg, Braunschweig/Wiesbaden 1992, p. 251.
- [19] G. Mackh, W. Ossau, D.R. Yakovlev, R. Hellmann, E.O. Göbel, T. Wojtowicz, G. Karczewski, J. Kossut, G. Landwehr, *Acta Phys. Pol. A* **88**, (1995), Proc. of this Conf. (Part II).
- [20] T. Wojtowicz, G. Karczewski, A. Zakrzewski, M. Kutrowski, E. Janik, E. Dynowska, K. Kopalko, J. Kossut, *Acta Phys. Pol. A* **87**, 165 (1995).
- [21] R.C. Miller, A.C. Gossard, D.A. Kleinman, O. Montenau, *Phys. Rev. B* **29**, 3740 (1983).
- [22] M. Kutrowski, G. Karczewski, P. Kossacki, Nguyen The Khoi, J.A. Gaj, J. Kossut, T. Wojtowicz, unpublished.
- [23] M. Sawicki, T. Dietl, T. Skośkiewicz, G. Karczewski, T. Wojtowicz, J. Kossut, *Acta Phys. Pol. A* **88**, (1995), Proc. of this Conf. (Part II).
- [24] D.D. Awschalom, J.M. Hong, L.L. Chang, G. Grinstein, *Phys. Rev. Lett.* **59**, 1733 (1987).
- [25] M. Dahl, A. Merlager, T. Litz, A. Waag, T. Wojtowicz, G. Karczewski, M. Sawicki, J. Kossut, unpublished.
- [26] A.K. Zakrzewski, L. Dobaczewski, T. Wojtowicz, J. Kossut, G. Karczewski, *Acta Phys. Pol. A* **88**, (1995), Proc. of this Conf. (Part II).
- [27] J. Jaroszyński, J. Wróbel, M. Sawicki, T. Skośkiewicz, G. Karczewski, T. Wojtowicz, J. Kossut, T. Dietl, E. Kamińska, E. Papis, A. Piotrowska, *Acta Phys. Pol. A* **88**, (1995), Proc. of this Conf. (Part II).
- [28] M. Sawicki et al., unpublished data.
- [29] K. Ando, H. Akinaga, *J. Magn. Magn. Mater.* **140-144**, 2029 (1995).